

REPORT DOCUMENTATION PAGE			Form Approved OMB No. 0704-0188		
Public reporting burden for this collection of information is estimated to average 1 hour per response, including the time for reviewing instructions, searching existing data sources, gathering and maintaining the data needed, and completing and reviewing the collection of information. Send comments regarding this burden estimate or any other aspect of this collection of information, including suggestions for reducing the burden, to Department of Defense, Washington Headquarters Services, Directorate for Information Operations and Reports (0704-0188), 1215 Jefferson Davis Highway, Suite 1204, Arlington, VA 22202-4302. Respondents should be aware that notwithstanding any other provision of law, no person shall be subject to any penalty for failing to comply with a collection of information if it does not display a currently valid OMB control number. PLEASE DO NOT RETURN YOUR FORM TO THE ABOVE ADDRESS.					
1. REPORT DATE (DD-MM-YYYY) 23-09-2002		2. REPORT TYPE Final Report		3. DATES COVERED (From – To) 01-Jun-00 - 01-Jun-02	
4. TITLE AND SUBTITLE DYNAMIC VISIBLE-TO-INFRARED CONVERTER			5a. CONTRACT NUMBER STCU Registration No: P-044		
			5b. GRANT NUMBER		
			5c. PROGRAM ELEMENT NUMBER		
6. AUTHOR(S) Professor Volodymyr Maluyutenko			5d. PROJECT NUMBER		
			5d. TASK NUMBER		
			5e. WORK UNIT NUMBER		
7. PERFORMING ORGANIZATION NAME(S) AND ADDRESS(ES) Institute of Semiconductor Physics, Ukrainian Academy of Sciences 45 Pr Nauki Kyiv 252650 Ukraine			8. PERFORMING ORGANIZATION REPORT NUMBER N/A		
9. SPONSORING/MONITORING AGENCY NAME(S) AND ADDRESS(ES) EOARD PSC 802 BOX 14 FPO 09499-0014			10. SPONSOR/MONITOR'S ACRONYM(S)		
			11. SPONSOR/MONITOR'S REPORT NUMBER(S) STCU 00-8003		
12. DISTRIBUTION/AVAILABILITY STATEMENT Approved for public release; distribution is unlimited.					
13. SUPPLEMENTARY NOTES					
14. ABSTRACT This report results from a contract tasking Institute of Semiconductor Physics, Ukrainian Academy of Sciences as follows: Semiconductor based pixel-less Dynamic Infrared Scene Projector (DISP) successful in generating of high-speed (microseconds range) broad band (3-16 microns) IR scenery is to be developed both theoretically and experimentally. For this purpose non-equilibrium thermal emission of semiconductors in the spectral range beyond the fundamental absorption region provoked by the band-to-band photogeneration of excess carriers (visible pumping) will be utilized for the first time (visible-to-infrared conversion). Such performance capabilities as maximum simulated temperature, noise equivalent temperature difference, dynamic range, spatial resolution of converted images and rise-fall time will be estimated and measured. The device prototype made of Ge will be tested in the Ukraine and USA. By the end of the work a Ukrainian patent will be requested, scientific paper will be submitted to the international journal and results reported at the international conference.					
15. SUBJECT TERMS EOARD, Physics, Solid State Physics					
16. SECURITY CLASSIFICATION OF:			17. LIMITATION OF ABSTRACT SAR	18. NUMBER OF PAGES 33	19a. NAME OF RESPONSIBLE PERSON Alexander J. Glass, Ph. D.
a. REPORT UNCLAS	b. ABSTRACT UNCLAS	c. THIS PAGE UNCLAS			19b. TELEPHONE NUMBER (Include area code) +44 (0)20 7514 4953

DYNAMIC VISIBLE-TO-INFRARED CONVERTER

**Partner Project P-044
between
The Science and Technology Center in Ukraine
and
Institute of Semiconductor Physics, Nat. Acad. of Sci. (Ukraine)
and
European Office of Aerospace Research and Development (USA)**

April 2000-June 2002

Project Manager Prof. V. Malyutenko

FINAL REPORT

**Distribution A:
Approved for Public Release
Distribution is Unlimited**

**Kiev
September 1, 2002**

Contents

Abstract	2
1. Introduction (The objective of the work)	3
2. Physical background	
2.1 Basic relationships	4
2.2 Free electrons and holes as an active body of DISP	5
2.3 Optimizing the parameters of DISP	6
2.4 Down conversion and optical gain. Is it possible?	9
3. Details of experimental facility and scene technology	
3.1 Experimental test systems and set ups	10
3.2 Technology of DISP screen	13
4. Results of DISPs tests and discussion	
4.1. Rise-fall time versus temperature	16
4.2. Spectral distribution of power emitted	17
4.3 IR integral power versus temperature and excitation level	17
4.4. Thermal principle of photon multiplication	20
4.5. 2D demonstration of IR images projected by the DISP	20
4.6. 3D DISP device concept	23
4.7. Patent pending	24
4.8. Independent testing, reporting, and publishing the results	25
5. Conclusion. Looking ahead	26
6. Acknowledgment	28
7. References	29

Abstract

Pixel less high temperature ($T > 500\text{K}$) Dynamic Infrared Scene Projector (DISP) successful in generating high-speed (microsecond range) broadband (3-16 microns) IR scenery through shorter wavelength pumping of DISP semiconductor scene ('visible'-to-infrared conversion) was developed, fabricated, tested and patented. New device operation principle based on theory of thermal emission and the results of experimental study are reported for the first time. Key parameters of new device prototype (based on Ge scene) are compared to that of modern conventional DISP engine (SBIR Emitter Array Projector). Proposals for the problem future study targeted at commercialization of the device are also outlined.

Keywords: dynamic IR scene projector, visible to infrared conversion, 8-12 μm spectral range, semiconductors, Ge, Si, free carrier photo generation, non-equilibrium thermal emission, free carrier absorption, spectral measurements in IR, carrier life time measurements, intraband electron transitions, dynamically modulated apparent temperatures, pixel less scene, positive and negative thermal contrasts, test targets for IR, 2D IR imaging, optical gain, photon multiplication, optical transistor, semiconductor DISP versus conventional DISP engine, patent pending.

Introduction

The capability for generating ground based realistic infrared (IR) scenery is becoming an increasingly important requirement for the testing and calibrating of infrared devices. The point is that the cost and complexity of conventional infrared systems require reducing the number of different type outdoor tests needed for critical program decisions. Moreover, such-large scale field tests do not offer repeatability or controllability of test conditions. For these reasons, since the early 1990's there has been a major progress in developing the Dynamic Infrared Scene Projector (DISP). DISP appears to be the primary element of any Hardware-in-the-Loop Simulator available (f.e. at National Institute of Standards and Technology, MD; University of Central Florida, Georgia Inst. Of Technology, University of Rochester, and University of Arizona who do research in infrared technologies).

To now a number of different DISP technologies have been investigated and treated¹. These are emissive (thin films, bridge or suspended membrane resistors), transmissive (liquid crystals, galvanic cells), reflective (deformable mirror or membrane cells, spatial light modulators) projectors, as well as laser scanners of different types. At the current time, the only emissive projectors based on the advanced suspended membrane resistor arrays, together with the laser diode array projectors, appear to be leading the DIRSP field. However, broadband thermal resistor arrays suffer from low time constant (beyond some milliseconds) and power dissipation capability, whereas narrow band laser arrays are limited to those applications where monochromatic projection is acceptable. Moreover both these DISP classes utilize pixel technology and this results in a low fill-factor value ($F < 0,5$ for small pixel area).

In this connection, the objective of this work is to investigate new approach toward the development of dynamic IR scene simulation technology. **The primary goal is to develop, fabricate and test pixel less ($F=1,0$) high temperature ($T > 500C$) DISP element successful in generating of high-speed (microseconds range) broadband (3-16 microns) IR scenery.** Non-equilibrium thermal emission of semiconductors is utilized for this purpose for the first time. The point is that the value of semiconductor thermal emission (TE) power in the spectral range beyond the fundamental absorption region is strictly affected by current carrier concentration (due to so-called free carrier absorption). As the result of band-to-band photo generation of excess carriers (visible pumping), the mentioned above TE value increases up to that for the black body value (with allowance for reflectivity) at given temperature. (In the words, free carrier absorption provokes semiconductor emissivity increase over the whole IR spectral range). It should be mentioned that, the first, the maximum TE modulated power falls into the near and mid IR (3-20microns). The second, this device time response is originated rather by free carrier recombination-generation processes (microsecond range) in the semiconductor scene but not by the Joule heating and cooling processes (millisecond range) which are dependent on a pixel thermal mass and thermal conduction. Also it should be mentioned, that predicted maximum apparent temperature values are limited only by the semiconductor melting temperatures (above 1000C). Moreover, 2D spatial resolution of the scene is limited by free carrier diffusion processes (1-25 um) contrary to 50 um pitch size of conventional discrete thermal resistor arrays. In conclusion, there are any driving electronics that demands large cumulative current and power and decreases the device fill factor.

What follows below is the summary of two-year long study, which was performed in the Institute of Semiconductor Physics in Kiev (Ukraine) for AFRL (USA)

1. Physical Background

2.1 Basic relationships

Consider a semiconductor plate ($0 \leq x \leq d$) with a reflection coefficient R (taken to be the same over the whole spectrum), absorption coefficient K (that can be dependent of the coordinate). The semiconductor temperature T differs from the background temperature T_g .

The total spectral power of the heat flux from the unit surface ($x = 0$) area with the allowance for multiple reflections is determined by the expression²

$$P_{\omega}^{tot} = P_{\omega} + RJ_{\omega}(T_g) + \frac{\eta(1-R)^2}{1-R\eta} J_{\omega}(T_{\omega}) \quad (1)$$

Where the second and third terms are the reflected and crystal-traversed background emission fluxes and the first term characterizes spontaneous TE of the plate,

$$P_{\omega} = \frac{(1-R)(1-\eta)}{1-R\eta} J_{\omega}(T) = \varepsilon J_{\omega}(T), \quad (2)$$

In expressions (1,2)

$$\eta = \exp\left(-\int_0^d K(x)dx\right) \quad (3)$$

is the factor of light transmission (transparency) through the plate and $J_{\omega}(T)$ is the spectral power of the blackbody TE (the well-known Planck distribution)

$$J_{\omega}(T) = \frac{\hbar\omega^3}{4\pi^2 c^3} \left(\exp\frac{\hbar\omega}{k_B T} - 1\right)^{-1} \quad (4)$$

Thus, the spontaneous TE of the plate is the product of two factors, namely, $J_{\omega}(T)$ and the emissivity factor $\varepsilon = (1-R)(1-\eta)(1-R\eta)^{-1}$ whose spectral dependence determines the TE features of actual bodies. It is seen in particular from the expression (2), that for actual bodies the TE power is below that of the blackbody. In two limiting cases, of low ($Kd \ll 1$) and high ($Kd \gg 1$) absorption values, it is of the form

$$\begin{aligned} P_{\omega}^{\min} &= KdJ_{\omega}(T), \\ P_{\omega}^{\max} &= (1-R)J_{\omega}(T). \end{aligned} \quad (5)$$

The case of high ($Kd \gg 1$) absorption is not of practical importance, since the TE spectral distribution is almost the same as that of the black body. Contrary to this, in the case of low ($Kd \ll 1$) absorption value, both the TE spectrum and integral power emitted are determined, to a great extent, by the value and the spectral dependence of the absorption coefficient K .

In summary, by modulating in any way the value of the plate (scene) absorption coefficient, the remarkable change of this scene TE value can be provoked. The favorable conditions for the process are initially transparent and therefore non-radiating scene ($Kd \ll 1$), negligible reflection ($R \rightarrow 0$), and

external factor capable to provoke this scene dynamic opaqueness ($Kd \gg 1$). Besides, the scene temperature (which is kept constant) well exceeds the background temperature ($T \gg T_g$). In this case, the scale of modulated power takes the form

$$P_{\omega}^{\max}/P_{\omega}^{\min} \approx (Kd)^{-1} \quad (6)$$

The theoretically possible maximum values of IR power emitted by the scene operated in induced non-transparency mode are shown in Fig1. As a matter of fact, these values are the blackbody integral power emitted in two spectral ranges (atmosphere transparency windows). These rather reasonable values say for themselves.

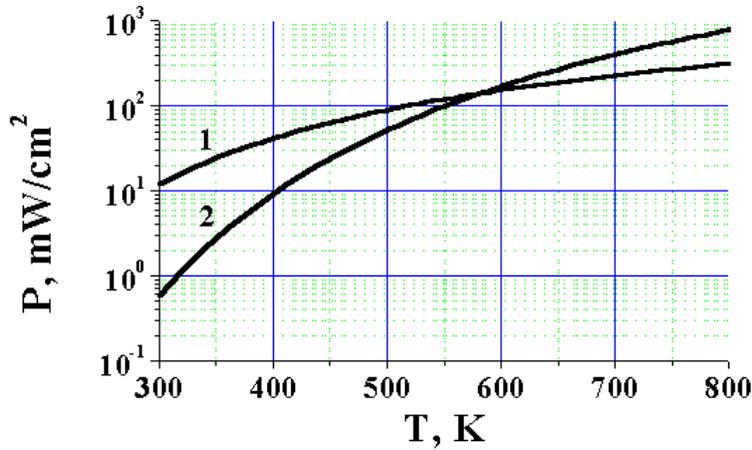


Fig.1. Maximum values of the TE power provoked by dynamic opaqueness of the scene in 3-5 μm (2) and 8-12 μm (1) spectral range (with allowance for scene reflection).

2.2 Free electrons and holes as active media of DISP

It is free carrier absorption range ($\hbar\omega < E_g$, E_g is material forbidden gap value) where absorption coefficient depends on current carrier parameters and therefore the TE value can be affected by modulation of free carrier concentration (n). Really, the absorption coefficient in this spectral range is connected to free electron and (or) hole concentration $K = \sigma_n n$ (σ_n is absorption cross-section of a quantum of given frequency ω by free electron). Thus, photo excitation of the scene with quanta energy of $\hbar\omega > E_g$, that increases the n value regarding to n_0 ($\Delta n = n - n_0$), results in modulation of TE power of a thin semiconductor scene in the longer wavelength spectral range ($\hbar\omega < E_g$, down conversion, see fig.2)

$$\frac{\Delta P_{\omega}}{P_{0\omega}} = \frac{\bar{n} - n_0}{n_0}, \quad \bar{n} = \frac{1}{d} \int_0^d n(x) dx, \quad (7)$$

$$P_{0\omega} = d \sigma_n n_0 [J_{\omega}(T) - J_{\omega}(T_g)],$$

At low excitation level ΔP_{ω} versus Δn linear dependence is valid. Further increase of pumping power provokes remarkable increase of free carrier concentration, gradual opaqueness of the scene and saturation of the TE power value P_{ω} to that for the blackbody kept at the same temperature.

It is important to stress that the TE power in the longer wavelength range depends not only on the scene temperature. It also depends on the integral value of light transmission factor (3) that can be modulated both by material parameters (d , R) and external factors (in particular, by power of visible light generating excess non-equilibrium charge carriers). Thus, the photo excitation of local scene area by the visible light (projected image) provides landscape picture in the IR (well beyond the fundamental absorption range). Lateral diffusion processes of free carriers limit the 2D spatial resolution of non-equilibrium IR image whereas carrier lifetime (τ) is responsible for the rise-fall time of this image. It is interesting to point out that free carrier parameters can be controlled through internal (impurity doping, plate thickness, surface processing) and external (temperature, power of visible light) factors. As it is seen from (5), the maximum modulated TE power can be achieved in initially optically thin ($K_0 d \ll 1$) element provided the visible pumping is capable to provoke its dynamic opaqueness ($Kd \gg 1$).

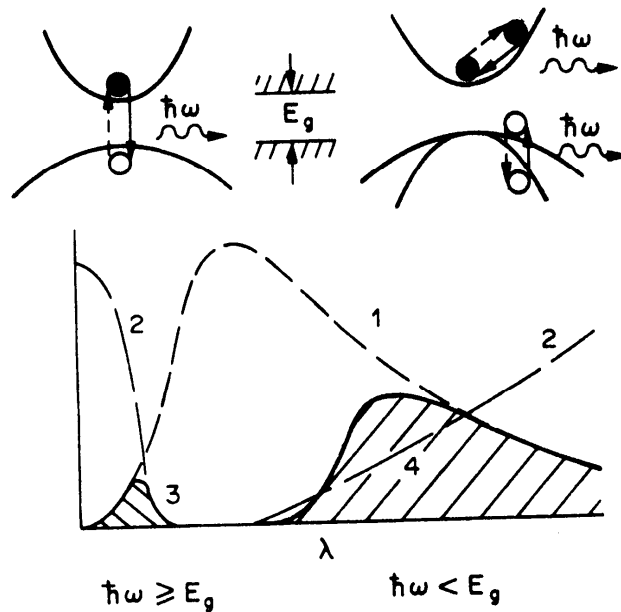


Fig.2. Energy band structure of a semiconductor and types of transitions in question. 1-the TE spectrum of black body; 2-spectral dependence of the absorption coefficient; 3,4- TE regions of charge carriers. It is the region 4 to be responsible for IR power emitted. Interband electron transitions provoked by photo excitation in region 3 create free electrons and holes. Intraband transitions in conduction band and valence band generate non-equilibrium IR TE of interest in region 4.

In summary, down conversion of visible light (i.e. the conversion of band-to-band external pumping ($\hbar\omega > E_g$) into non-equilibrium TE in the IR spectral range of free carrier absorption ($\hbar\omega < E_g$) appears to be new promising principle of pixel less DISP. The fundamental process inside this principle is dynamic modulation of scene emissivity ε provided it is initially transparent in the IR ($Kd < 1$). By this reason, the scene materials are not limited by direct band gap semiconductors.

2.3 Optimizing the parameters of the IR scene

Consider a semiconductor plate (scene) which thickness d is comparable to the diffusion length (L) of charge carriers ($d \leq L$). The plate is pumped by radiation with the frequency $\omega \geq E_g/\hbar$, and this

results in free electrons and holes increase. Each photon passing through unit surface (1cm^2), increases non-equilibrium free carrier concentration by $\Delta n = \tau d^{-1}(1-R)$, where τ is the lifetime of electron-hole pairs. In order to calculate corresponding increase of absorption coefficient $\Delta K = (\sigma_n + \sigma_p)\Delta n$ and dynamic TE value (see eq.7) we need real spectral dependencies of electron and holes cross-sections in IR spectral range of interest (say $3\text{-}5\ \mu\text{m}$ or $8\text{-}12\ \mu\text{m}$). As an example, the spectral dependence of hole cross section in Ge is shown in Fig.3 whereas the same for electrons has more simpler form ($\sigma_n \sim \lambda^2$). For many estimates however the spectral dependence of both cross sections may be neglected provided the spectral range of interest is rather narrow (like transparency windows mentioned above). The real values of electron and hole cross-section measured at $\lambda = 10,6\ \mu\text{m}$ are listed in Tabl.1.

At higher temperatures ($T > 300\text{K}$), both electrons and holes are responsible for absorption coefficient value as semiconductors (like Ge or Si) become intrinsic ($n_0 = p_0$). As it is practically always valid, however, the hole absorption cross section exceeds the same for electrons ($\sigma_p \gg \sigma_n$). For example⁴, in Ge at 300K $\sigma_p = 68 \cdot 10^{-17}\ \text{cm}^2$ whereas $\sigma_n = 4 \cdot 10^{-17}\ \text{cm}^2$ at $\lambda = 10,6\ \mu\text{m}$. As a result, it is the hole component to be responsible for IR thermal emission value. Thus, reducing the hole concentration to produce minimum initial TE power of the scene (see eqs.5, 6) should be performed by intentional scene n-type doping ($N_d > N_a$). As the intrinsic concentration of carrier n_i ($n_i^2 = n_0 p_0$) depends on the material temperature, then the optimum n-doping level appears to be temperature dependent value also.

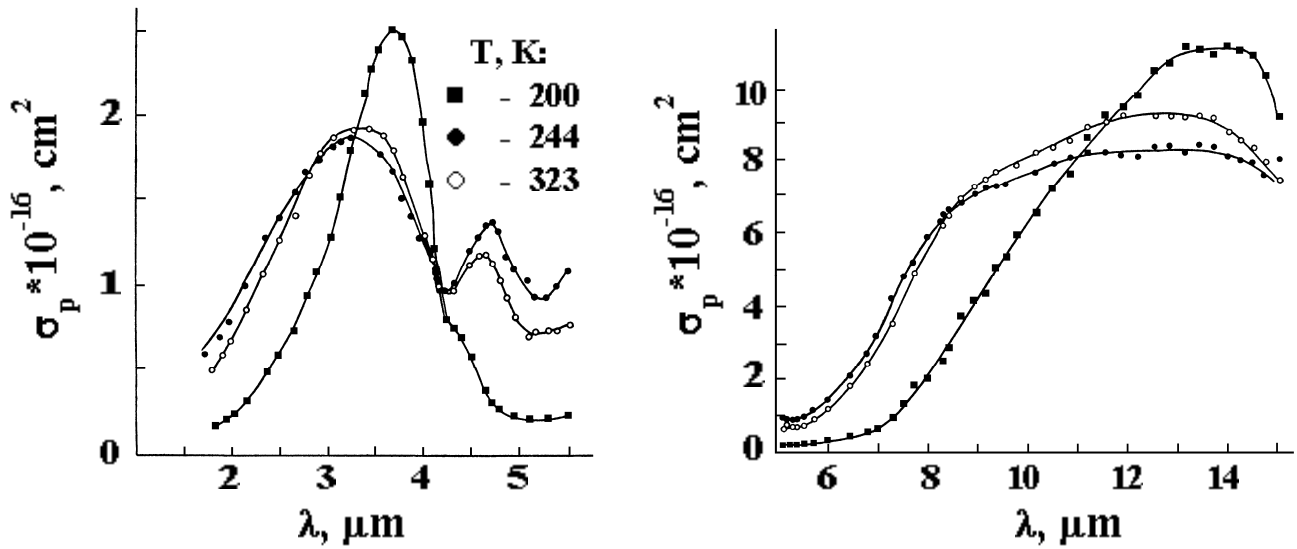


Fig.3. Spectral dependencies of absorption cross-section for holes in Ge at different temperatures [3]. Two maximums in $3\text{-}5\ \mu\text{m}$ range are connected to direct transition between sub bands of heavy and light holes whereas the plateau in longer wavelength range is due to direct transition between degenerated sub bands of heavy holes and non-direct transitions inside these sub band.

The temperature dependence of absorption coefficient in Ge of different doping levels is shown in Fig.4. As one can see, low temperature scene ($T < 300\text{K}$) may be practically undoped. The $450 > T > 350\ \text{K}$ range demands slightly doped Ge whereas the scenes operated at higher temperatures ($T > 450\text{K}$) should be highly doped. While calculating results presented in Fig.4 it was assumed for the simplicity that $\sigma_p/\sigma_n = \text{const}$ whereas lattice absorption was neglected.

Achieving high temperature transparent scene is a compromise between doping level N_d and intrinsic carrier concentration n_i . Exponential growth of n_i value with temperature increase

determines upper temperature limit of Ge scene. Really, as one can see in the Fig.4, the 300 μ m thick Ge plate can be considered as practically transparent at T<450K (Kd<1 relation is valid).

Table 1. Absorption cross-sections at 10,6 μ m⁴

Material	$\sigma_n \cdot 10^{17}, \text{cm}^2$	$\sigma_p \cdot 10^{17}, \text{cm}^2$	n_i, cm^{-3} (at 300 K)
Si	9	35	$1,5 \cdot 10^{10}$
Ge	4	68	$2,5 \cdot 10^{13}$
InSb	3	86	$2 \cdot 10^{16}$
InAs	6	35-65	$8 \cdot 10^{14}$
GaAs	5	50	$\approx 10^8$
Te	–	90	$\approx 4 \cdot 10^{15}$
PbS	≈ 5	≈ 25	$\approx 10^{15}$
PbTe	≈ 3	≈ 20	$\approx 10^{16}$
GaP	40	–	≈ 1
SiC	150-270	–	$< 10^{-6}$

. The DISP efficiency depends on how many excess carriers the pumping source can generate. Therefore, the carrier lifetime (τ) is a key parameter of DISP scene. Really, the higher this value the lower pumping power value could remarkably increase carrier concentration and simulate IR dynamic picture. When it comes to moderately doped Ge at T>300K, the values of 100 μ s and higher look reasonable provided surface recombination process is neglected. If this is not the case the effective carrier lifetime τ_{eff} depends on the volume lifetime τ_v and surface recombination velocity s value

$$\tau_{\text{eff}} = 1 / (1/\tau_v + 2s/d) \quad (8)$$

It should be noted however that there is trade off between the simulated dynamic apparent temperature value and rise-fall time of the IR picture DISP simulates. Really, the higher lifetime the higher carrier concentration created by the same power of visible light.

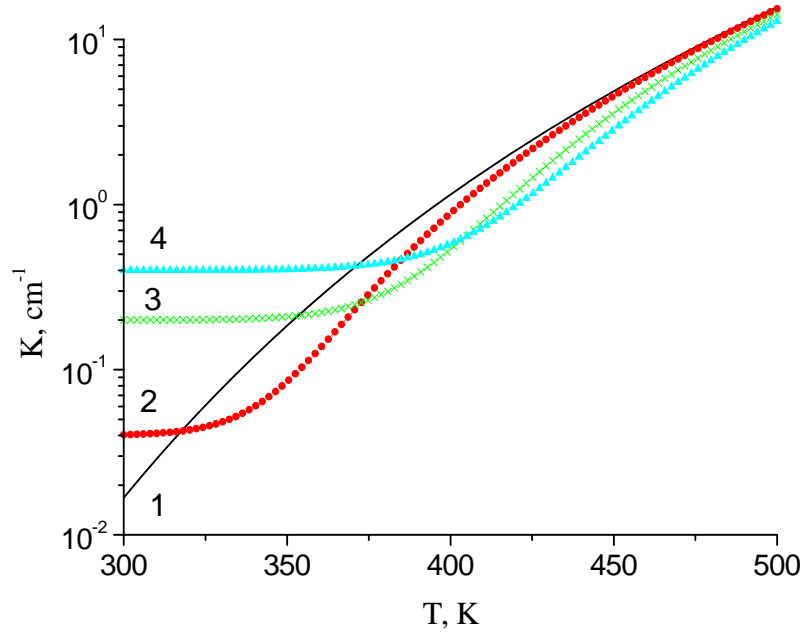


Fig.4. Absorption coefficient $\lambda=10,6\mu\text{m}$ of Ge scene vs temperature for different doping levels: 1 – intrinsic material, 2 – $N_d = 1.10^{15}$, 3 – $N_d = 5.10^{15}$, 4 – $N_d = 1.10^{16} \text{ cm}^{-3}$. N-doping results in higher scene transparency at higher temperatures.

The impact of unauthorized heat sources at DISP performance follows from eq.1. Initially transparent and therefore low radiating scene is affected by both reflected and crystal-traversed background emission. Using cooled chamber would minimize background radiation impact and increase the range of simulated by the DISP apparent temperatures.

The maximum power emitted is limited by the DISP scene temperature and reflectivity of IR scene in the spectral range where blackbody radiation is centered. This demands for transparency coating of surface through which the IR radiation escapes. It should be remembered that the scene IR emission is two sided, but the backside-escaping radiation may be reflected toward the front plane to enhance the total forward emission. The coating may be tuned to minimize the reflection coefficient R in 3-5 μm , 8-12 μm or 3-12 μm spectral ranges.

In summary, the emissivity increase of optically thin DISP element followed by the increase of IR power emitted is a direct effect of non-equilibrium free carrier generated by the visible pumping. Free electrons and holes provoke the increase of absorption coefficient and the scene opaqueness in IR. Phonon assisted non-direct electron transitions in the conduction band and direct hole transitions between sub bands of the valence band forms different values of absorption cross sections ($\sigma_n < \sigma_p$). Several mW/cm^2 are typical values of dynamically modulated IR power emitted by the scene kept at high temperature ($T > 300\text{C}$). As an example, high-temperature ($300\text{K} < T < 500\text{K}$) DISP based on down conversion principle can be made of thin ($d \sim 300\mu\text{m}$) Ge scene intentionally n-doped ($N_d \leq 1.10^{16} \text{ cm}^{-3}$). The achieving for higher simulating temperatures demands for thinner scene and heavier doping level. Scene carrier lifetime should be as high as possible whereas surface recombination processes should be minimized. Besides, the front plane of the scene is covered with transparency coating capable to minimize reflection whereas the scene itself is kept in cooled chamber.

2.4 Down conversion and optical gain. Is it possible?

Really, is it possible to have more IR photons emitted by the scene as a result of down conversion than those emitted by the visible source and absorbed by this scene? Calculate the number of IR photons emitted by the semiconductor scene with the thickness equal by the order of magnitude to the diffusion length L . Non equilibrium TE is due to generation of electron-hole plasma by visible pumping with the frequency $\omega \geq E_g/\hbar$ (band-to-band excitation). Each photon passing through unit scene surface increases non-equilibrium pair concentration by $\Delta n = \tau L^{-1} (1-R)$. In turn, this process results in corresponding free carrier absorption coefficient increase by $\Delta K = (\sigma_n + \sigma_p) \Delta n$. The last means that the number of non-equilibrium TE quanta induced by one exciting photon can be written as

$$\Delta N = \int_0^{\infty} \frac{\omega^2}{4\pi^2 c^2} \left(e^{\hbar\omega/kT} - 1 \right)^{-1} \Delta K L d\omega \quad (9)$$

Suppose also that the excitation level is low $(K_0 + \Delta K)L \ll 1$, i.e. the optical thickness of the scene remains small (we have to remember that ΔN saturates at higher excitation level $(K_0 + \Delta K)L \gg 1$ and this case is not of importance for optical gain).. By substituting into (9) plasma parameters we obtain

$$\begin{aligned} \Delta N &= \int_0^{\infty} \frac{\omega^2}{4\pi^2 c^2} \left(e^{\hbar\omega/kT} - 1 \right)^{-1} (1-R) (\sigma_n + \sigma_p) \tau d\omega = \\ &= \int_0^{\infty} (1-R) N_{\omega} (\sigma_n + \sigma_p) \tau d\omega, \end{aligned} \quad (10)$$

where N_{ω} is the spectral distribution of the black body photon flux which can be calculated from the first principles. If one neglects the electron cross-section and spectral dependence of σ_p , the number of IR photons emitted by the semiconductor scene in response to single visible photon absorption (quantum conversion efficiency η_{phot}) can be written in simple form

$$\Delta N = (1-R) \sigma_p \tau \int_0^{\infty} N_{\omega} d\omega = 1.5 \cdot 10^{11} T^3 \sigma_p \tau (1-R) \quad (11)$$

The estimates for Ge scene ($\sigma_p = 6,8 \cdot 10^{-16} \text{ cm}^{-3}$ and $\tau = 10^{-3} \text{ s}$) show that the quantum conversion efficiency $\eta_{\text{phot}} > 1$ really can be achieved ($\eta_{\text{phot}} = 0,9; 7,0; 12,5$ and $21,5$ for $T = 300\text{K}, 400\text{K}; 500\text{K}$ and 600K).

The physical reason of photon multiplication as it follows from the eq.(11) is rather simple. The electrons and holes created by the visible pumping interact with the background IR photons and phonons, which numbers are determined by the scene temperature. The cross section values σ_n and σ_p determine the strength of this interaction. The duration of this electron-photon-phonon interaction depends on carrier lifetime τ_{rel} ($10^{-3} - 10^{-4} \text{ s}$) whereas electron and hole relaxation time τ is extremely short (of order $10^{-8} - 10^{-12} \text{ s}$, carrier scattering process). As each scattering process is capable to produce IR photon, then the average number of IR photons generated inside unit scene volume is $\sim \tau/\tau_{\text{rel}}$.

To calculate the energy conversion efficiency of the process we assume the incident quantum energy to be $\hbar\omega = E_g$ and average quantum energy of the black body emission to be $\hbar\omega_{\text{average}} = 2 \cdot 10^{-4} T \text{ eV}$. This gives for the energy efficiency coefficient the following estimate

$$\eta_{en} = \Delta N \frac{\hbar \omega_{average}}{\hbar \omega} = \Delta N \frac{2 \cdot 10^{-4} T}{E_g} \quad (12)$$

and makes the relation $\eta_{en} > 1$ valid at $T > 450$ K.

In summary, DISP element operating in down-conversion mode not only transform visible image into IR. It is very important, that this conversion process capable in principle to operate with both quantum and energy efficiencies beyond 100% (as a matter of fact DISP scene looks like optical transistor). The summary does not contradict to thermodynamic laws as the heater, which supports the scene at fixed temperature, has been delivering the additional energy. The favorable conditions for the process are maximum carrier lifetime ($\tau_n = \tau_p = \tau$), minimum carrier relaxation time, and higher temperatures of the scene.

2. Details of experimental facility and scene technology

3.1 Experimental test systems and set ups.

Carrier lifetime measurements

The carrier effective lifetime have been measured by analyzing the photoconductivity decay. The computer controlled experimental set-up consists of a pulse light source (flash lamp with maximum power emitted mostly in visible range, good for testing of the scene made of Ge and Si) with the pulse duration of 5 μ s and the repetition rate of some 0,5-1s. The voltage drop at the load resistor induced by modulation of crystal conductivity (caused by free carrier photo generation) is recorded and memorized by electronic recorder with 5 μ s time interval (step). Temperature controller and 'hot' chamber control and support the object temperature in $300K \leq T \leq 500K$ range. The set of optical filters permits the selective study of 'surface' and 'volume' type carrier generation process and thus the quality of scene surface treatment. The typical curves of photoconductivity decay are shown in Fig.5. The object is Ge scene with chemically etched surfaces. As one can see, surface oxidation at higher temperature decrease decreases effective carrier lifetime through enhanced surface recombination process.

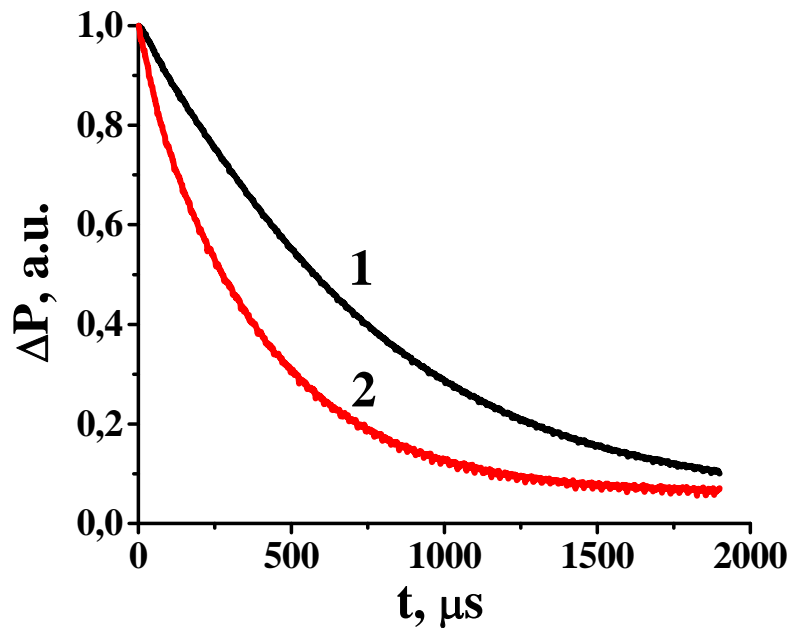


Fig.5. Photoconductivity relaxation curves in Ge scene ($d=3,5$ mm, $T= 373$ K) clearly indicate the impact of surface recombination process at the effective carrier lifetime. 1-scene surface is chemically etched, $\tau =800\mu\text{s}$; 2-scene was heated up to 450K and cooled down to 373 K in air, $\tau_{\text{eff}}=390\mu\text{s}$.

TE spectral distribution measurements

The TE spectra were measured automatically in the 8-12 μm spectral range. The key elements of the spectral test unit are shown in Fig.6. Visible light projector focused at front plane of the scene modulates the scene emissivity in IR whereas scene heater and temperature sensor control its temperature. Reflective type IR condenser focuses the TE escaping the back scene plane at spectrometer slit. The IR radiation spectra is recorded by pyroelectric detector (lithium niobate) and selective nanovoltmeter operated in lock-in mode. The mechanical chopper modulates the TE flux with the frequency of 5.8 Hz.

In order to measure the TE in absolute units rather than in arbitrary ones there was also measured the black body spectrum with using a copper plate covered with black and mounted on the sample place at crystal holder. Then the scene spectrum was normalized by the black body one to obtain the real scene emissivity spectrum.

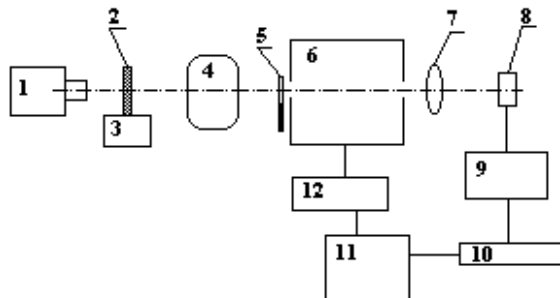


Fig.6. Experimental set-up for spectral measurements in IR.

1 – visible light source, 2 – DISP scene, 3 – heater and temperature controller, 4 – reflective type IR condenser, 5 – mechanical chopper, 6 – spectrometer, 7 –IR lens, 8 – pyroelectric detector of IR radiation, 9 – lock- in selective nanovoltmeter, 10 digital voltmeter, 11 – computer, 12 – spectrometer control unit.

The examples of the TE spectra measured in the range of free carrier absorption in Ge scene are show in Fig.7. It is interesting to note that these spectra behavior well correlates with the theory developed in Section 1. The first, IR TE exists in the spectral range of interest (well beyond the fundamental absorption range). The second, its value and spectral distribution are affected by initial transparency of the scene ($K_d < 1$ for curve 4 and $K_d > 1$ for curve 2). And the third, maximum TE value is equal to that for black body with allowance for $(1-R)$ factor (remind here, the maximum power emitted is limited by the DISP scene temperature and reflectivity in the spectral range where blackbody radiation is centered). Our further concern in this work will be dynamically controllable TE signal through modulation of free carrier concentration by external light.

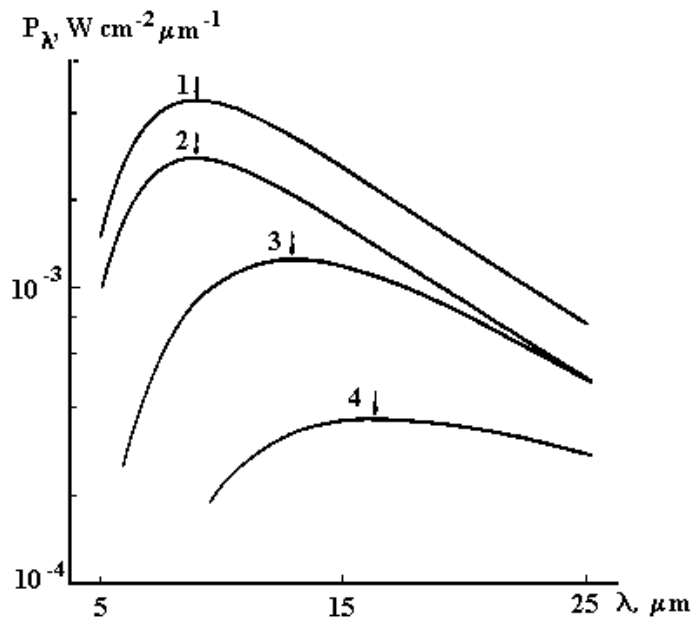


Fig.7. Thermal emission spectra of the black body (1) and Ge plates of various thickness and doping level (2-4) at 320 K. N_d-N_a (cm^{-3}): 2 – 1.5×10^{16} ; 3,4 – 1.2×10^{17} ; d (cm): 2 – 0.5; 3 – 0.1; 4 – 0.022. Arrows indicate positions of spectral dependencies maximums.

Conversion efficiency tests

The test system consists of the YAG-laser ($\lambda=1,06\mu\text{m}$, free generation mode, $120\mu\text{s}$ pulse duration) as the pumping source and registering head with pyroelectric (based on lithium niobate) detector sensitive to the integrated IR TE signals and preamplifier (see Fig.8). The laser power and IR signal pulse form were measured by coaxial photocell whereas pulse energy meter was used to calibrate both photocell and pyrodetector. This test system permits also “power emitted versus pumping power” measurements.

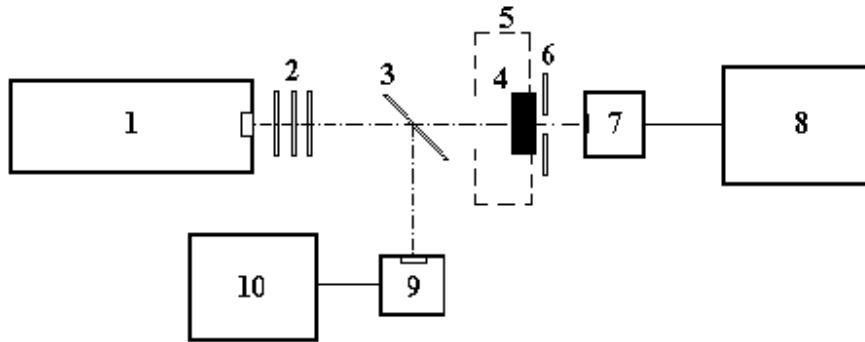


Fig.8. Experimental set-up for conversion efficiency measurements.

1 – YAG laser, 2 – optical attenuator, 3 – splitter of a laser beam (the 8 % reflection coefficient), 4 – sample, 5 – sample temperature controller, 6 – cold diaphragm, 7 – pyroelectric detector, 8 – storage oscilloscope, 9 – coaxial photocell, 10 – storage oscilloscope

Visualizing the converted image

The sketch of experimental set up is shown in Fig.9. Visible light ($h\nu > E_g$) projecting system focuses the target image on front side of semiconductor scene kept at given temperature ($T > T_g$). Calibrated thermal imaging camera (HgCdTe cooled photo detector, 8-12 μm spectral range) scans backside of the scene and maps the two dimensional (2D) emissivity pattern provoked by excess free carriers generated by visible light. Parameters of interest are apparent temperature (T_a) or IR power emitted (P) values-the signal differences between illuminated and shadowed scene. It is to mention, that the camera measures radiance differences but not temperatures, therefore, T_a and P values are connected by calibrated signal transfer function.

The frame exposition time can be varied from 400 μs (single line frequency) to 40 ms (full frame frequency). The 40 ms delay between frames permits real time investigation of dynamic map pattern with recording 25 frames per second and producing a TV-like real time false color image. Data acquisition and image processing are computer controlled. The parallel video channel equipped with a CCD camera permits easy positioning and focusing a scene along the system optical axis. The results are available either as apparent temperature or IR power.

The camera is synchronized with visible light pulse in such a manner that the picture of interest appeared at the second frame, whereas the first frame captured the background initial image. By subtracting these frames one can get apparent temperature difference ΔT maps provoked by free carriers. It was carefully verified that visible light pulse did not changed the real scene temperature.

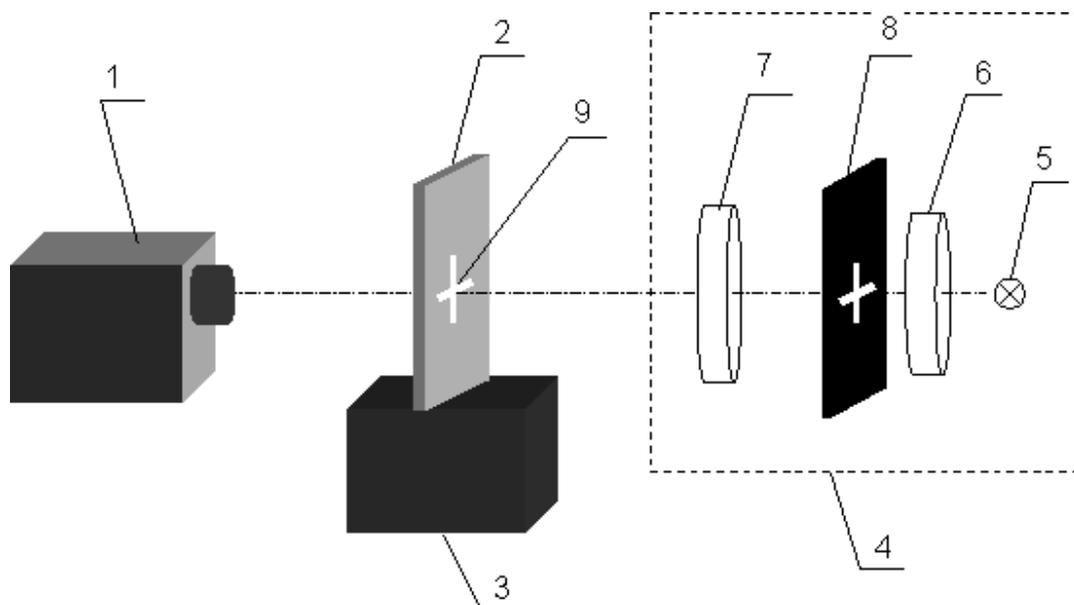


Fig.9. Visible-to-IR down conversion set up.

1–IR scanning camera, 2 – infrared scene (semiconductor –plate), 3 – heater (ceramic resistor and copper crystal holder) and temperature controller, 4 –target projector, 5 – 150 W incandescent lamp with tungsten filament, 6 – condenser (glass), 7 – lens (glass), 8 – target as a cross like cut, 9 – target image.

3.2 Technology of DISP screen

As it follows from Section 2 of this report, the scene of visible-to-IR converter should be made of a semiconductor with maximum values of free carrier lifetime τ and absorption cross sections σ_n or (and) σ_p at given temperature ($T > 300\text{K}$) and in given spectral range (3 to 5 μm or 8 to 12 μm). This material should be initially transparent at higher temperatures (see comments in Fig.10), its surface can be treated in simplest way to eliminate surface carrier recombination processes and minimize light reflection. Naturally this material should be cost effective.

By this reasons, as a starting material we had been testing Ge monocrystals thought some measurements were made with Si. Really, these non-expensive semiconductors are available of different doping levels and substrate dimensions. There is no problem with booking the sample with record values of carrier lifetime (some milliseconds). Standard chemical treatments permit smallest of known to date surface recombination velocity values ($s \leq 100 \text{ cm/s}$). High class optical polishing and technology of transparency coating does not cause the problem also.

Typical scene dimensions (surface area) were 1-2 cm^2 with a thickness of about 1mm to (which is comparable to the carrier diffusion length) and doping level relevant to the temperature of tests. However, the variety of scenes of different thickness, surface treatments and doping levels were tested also. Both semiconductor materials were grown in Ukraine.

As the technologies of polishing or etching Ge and Si scenes are well treated and described in the literature some comments only on the technology of transparency coating for Ge should be given below.

Remark: we have to note that only a few papers are published till now on surface properties of Ge and Si at higher temperature. By this reason, we have been treated the scenes by chemical, which have been used for getting small surface recombination velocity at room and lower temperatures.

Intrinsic carrier concentration in Ge and Si

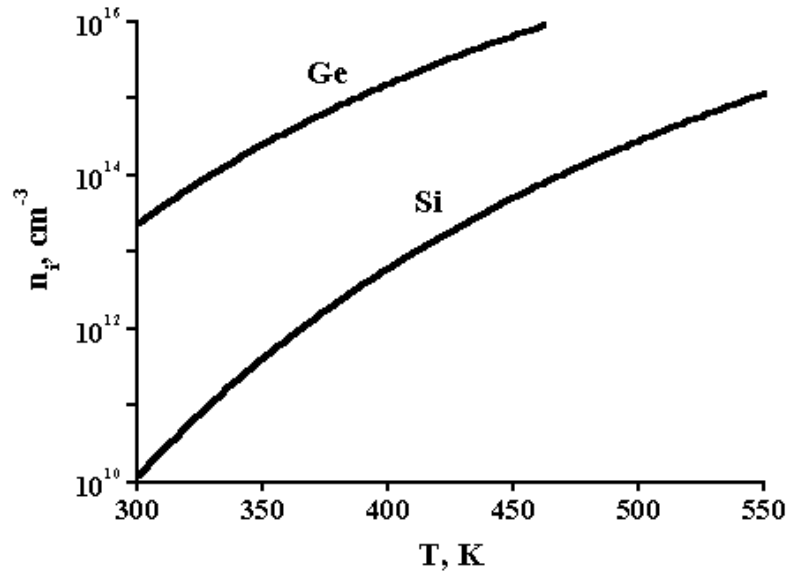


Fig.10. High rate of thermal generation of free carriers (n_i concentration) in Ge is responsible for initial remarkable absorption coefficient value at $T > 450\text{K}$ ($K > 1$) whereas the same for Si is low enough to make the material transparent even at $T = 550\text{K}$ ($K < 1$ with allowance for lattice absorption).

Germanium monoxide (GeO) was selected as an antireflection coating for n-Ge in the spectral range 8 to 12 μm . It is due the fact that this material is in fact transparent in this range. Moreover, the GeO film has the refraction index $n_{\text{GeO}} = 2.1$ that satisfies the condition $n_{\text{GeO}} = (n_{\text{Ge}})^{1/2}$ for getting minimum reflection at the interface film-Ge substrate. The coating is also attractive as it may be deposited by the vacuum evaporation technique at comparatively low temperatures ($T_{\text{ev}} < 1000\text{ }^\circ\text{C}$) unlike most dielectric coatings. The impact of GeO transparency coating at reflectivity of Ge scene is show in Fig.11. In some cases the scenes with CdSe transparency coating were tested also.

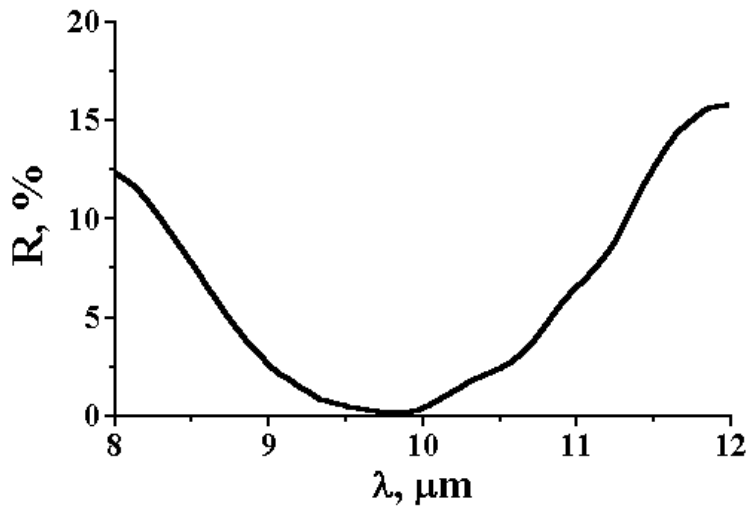


Fig.11. Spectral dependence of reflectivity of Ge scene covered with 1,2 μm thin GeO film. Initial Ge surface reflectivity is of some 36%.

4. Results of DISPs tests and discussion

4.1 Rise-fall time versus temperature

Time response of the visible-to-infrared converter is determined by the free carrier recombination-generation processes (a microsecond range) in the semiconductor scene rather than the Joule heating and cooling processes (millisecond range) which are dependent on a pixel thermal mass and thermal conduction. In this connection we have been measured temperature dependencies of carriers lifetime in typical Ge and Si slabs, which were used for the scene fabrication. The results of measurements are shown in Fig.12. They don't contradict in general to known published data. The fact is that the Shockley-Read process is responsible for carrier recombination in these materials. The values of carrier lifetime and its temperature dependence depend on the nature of recombination levels disclosed inside the material forbidden gap (so-called deep level recombination). One thing of common is that $\tau = f(T)$ dependence demonstrates non-monotonous curve, whose maximum position depends on these center nature. The lifetime values scatter in nanosecond-millisecond range and record values of order some milliseconds were reported. However, due to relation $\tau_n = \tau_p = \tau$ the carrier lifetime is limited by surface recombination processes.

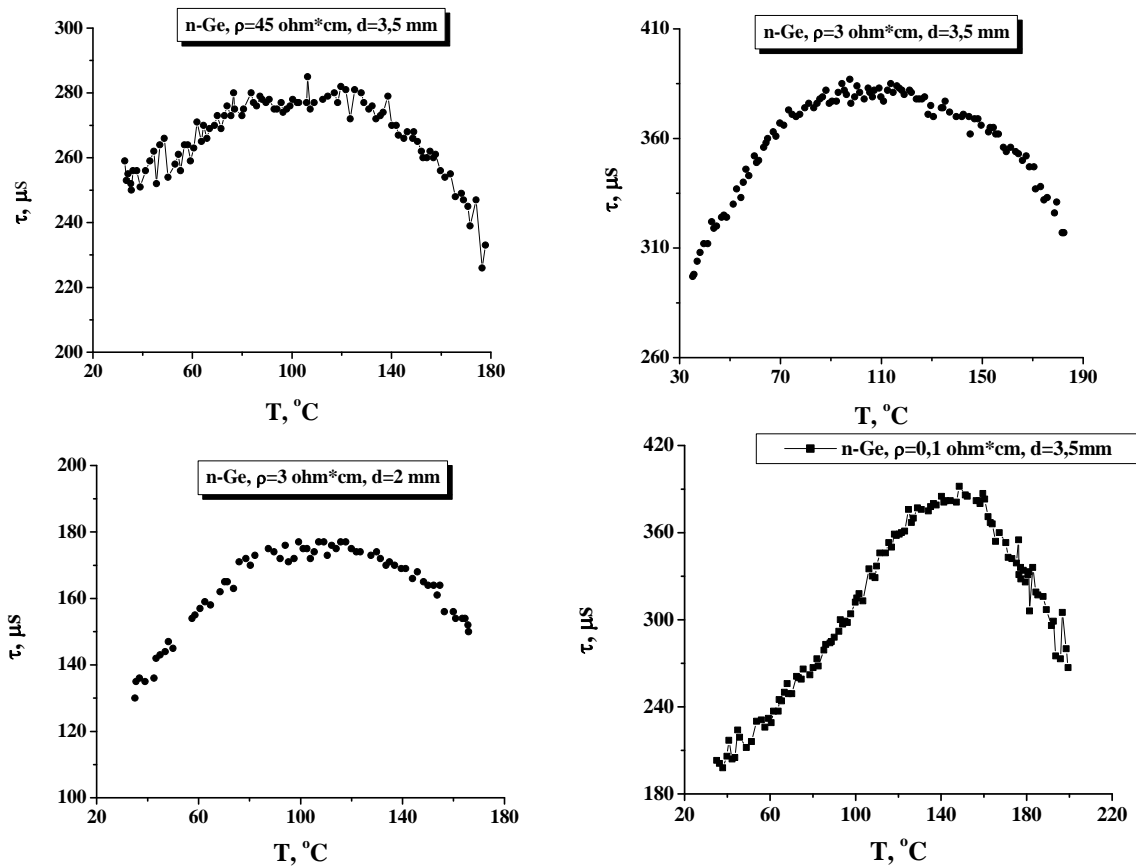


Fig.12. Lifetime versus temperature in Ge and Si of different thickness. Shown are: undoped Ge with intrinsic conductivity; slightly doped n-Ge (the effect of surface impact is clearly seen), and heavy doped n-Ge.

In summary, n-doped Ge scenes look promising for practical purposes. However, most promising slabs are only those with maximum τ values (some milliseconds), which we failed to book or test. Besides, the attention should be paid to scenes surface treatment, as this problem is not studied in details at high temperatures.

4.2. Spectral distribution of power emitted

The spectral distributions of the Ge scene emissivity ε measured at low level of visible light power are shown in Fig13. The spectra are measured for n-Ge ($\rho= 3 \text{ ohm}\cdot\text{cm}$, $d=3,5 \text{ mm}$) at $T=80 \text{ }^\circ\text{C}$. It is seen that excess carrier generation increases the scene emissivity in all IR range. It is very important also that the TE spectra are smoothly distributed in the 8-12 μ range with some details originated from the material band structure. In particular, the maximum at $\lambda=4-5 \mu\text{m}$ is connected to direct transition between sub-bands in the valence band (see Fig.3) whereas longer wavelength non-uniformity is due to lattice absorption⁵. By increasing temperature the scene emission shifts towards shorter wavelengths (like for the black body). The spectra were intentionally measured at low excitation level therefore the signals are remarkably lower than those for the blackbody and indicate "thin structure" mentioned.

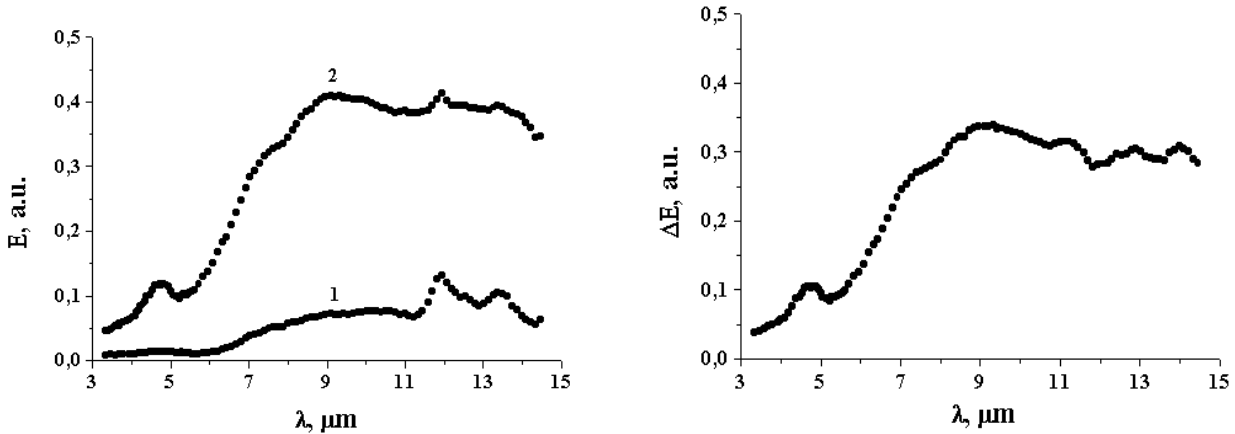


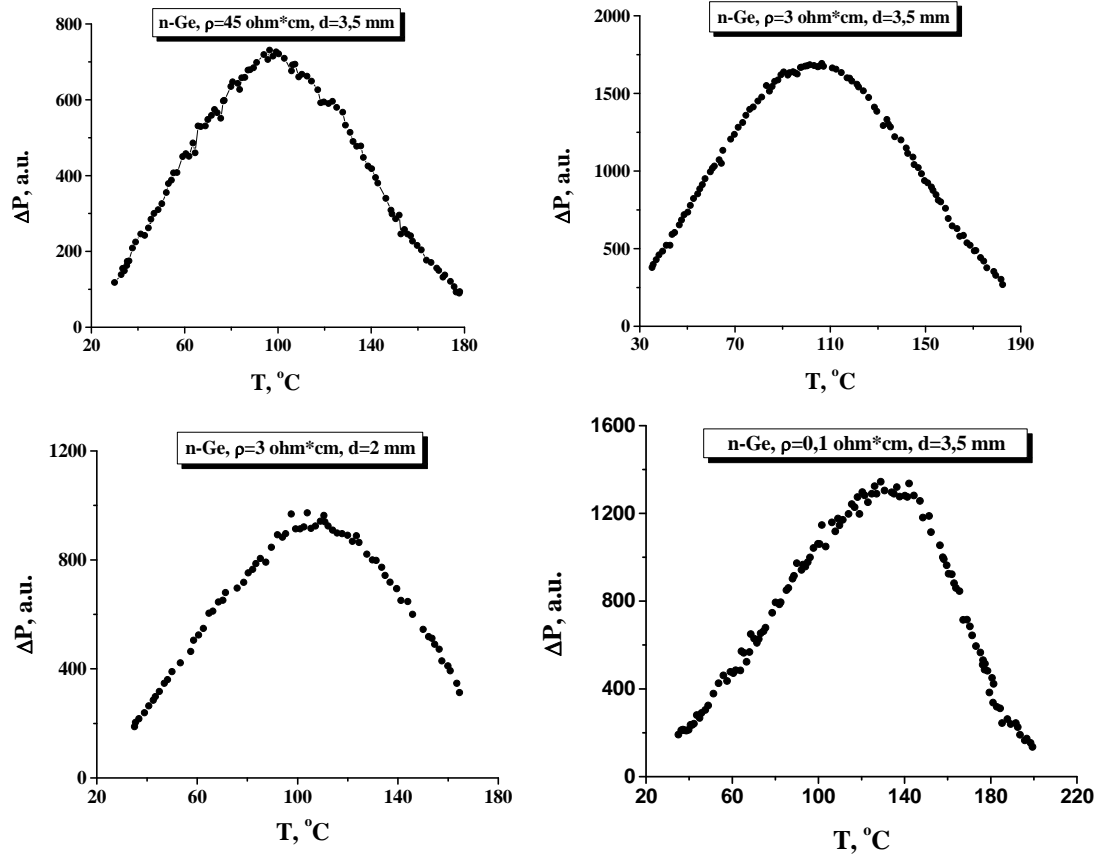
Fig.13 Typical spectral distribution of scene IR emissivity (see eq. 2). Sb doped Ge scene ($\rho= 3 \text{ ohm}\cdot\text{cm}$, $d=3 \text{ mm}$) is kept at $T=353\text{K}$. 1-initial spectrum of the scene $\varepsilon_{0\lambda}$; 2-the same for illuminated scene ε_{λ} ; left-dynamically modulated spectrum of the scene $\Delta\varepsilon_{\lambda}=\varepsilon_{\lambda}-\varepsilon_{0\lambda}$. Thin structure is result of low excitation level.

In summary, the spectrum of DISP scene is similar to that for the black body in 8-12 μm range. This advantage make the device more attractive for DISPs system compared to LEDs or laser array, whose spectra are narrowed around given wavelength and never cover the ranges of IR thermal imaging cameras.

4.3 IR integral power versus temperature and excitation level

Temperature dependencies of integral power emitted are shown in Fig. 14 for several Ge scenes of different doping. YAG laser or flash lamp created non-equilibrium carriers and TE and IR

TE signal was detected by HgCdTe cooled photo detector (11 μ m cutoff wavelength). Really, the doping level drastically affects the optimum scene temperature (compare first and last figures). Moreover, the strange fact is the 140C cutoff temperature for heavy doped scene (the “hot” result:



we registered 200C cutoff for this scene provided its thickness is of 0,4mm).

Some remarks on the cupola-like form of $\Delta P=f(T)$ dependencies. The higher temperature of initially optically thin scene the more IR power this scene generate in response to carrier

Fig.14. Temperature dependencies of dynamically modulated TE integral power for Ge scene of different thickness and doping levels. The striking result is the possibility to tune the temperature optimum from 95C in intrinsic material to 140C in heavy n-doped material.

generation process even at constant power of visible pumping (see factor $J_{\omega}(T)$ in eqs.2,4). Due to thermal generation, equilibrium carrier concentration increases exponentially with temperature increase therefore the scene initial emissivity ϵ_0 also increases (see eq.7, slightly scene opaqueness). As the excitation level fixes final value of opaqueness, then the value of its dynamically modulated part $\Delta\epsilon$ decreases. This process is difficult to avoid, as the Plank's factor is proportional to the temperature in IR spectral range whereas thermal carrier generation exponentially depends upon the temperature.

As a real scene emissivity never exceeds that for the black body, it is easy to predict the saturation of IR TE power versus visible pumping level dependence (see Fig.15). Naturally it is assumed that visible pumping does not increase the scene temperature. Also it is clear from the said above, the higher temperature of test the higher saturation level of TE signal occurs.

Dynamic opaqueness, which happens at high excitation level, is responsible for new phenomenon what we called optical memory. The point is that from the common point of view the TE signal has to start relaxing immediately after the pumping source is switched off. It is not the case however for high excitation levels capable of producing dynamic scene opaqueness. In

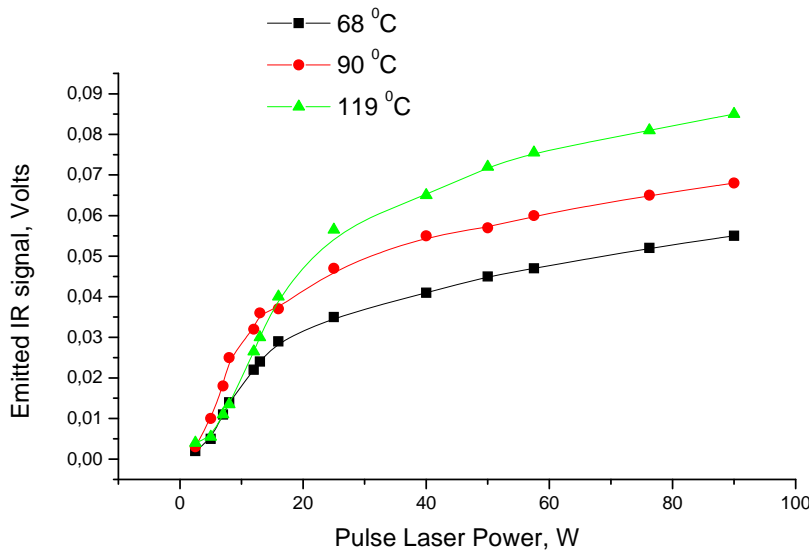


Fig.15. TE power versus pumping level dependence clearly indicates saturation process, which is due to induced dynamic opaqueness of the scene. Plank's factor is responsible for the increase of saturation level with temperature increase.

this case, the level of TE maximum value remains stable as long as the scene remains opaque ($Kd > 1$). The decrease of TE power starts some later and relates to the situation when the relation $Kd \leq 1$ enters the force what in turn is due to carrier recombination process. Fig.16 illustrate this phenomenon. What shown is the relaxation process of IR TE provoked by excitation of YAG laser with pulse duration of $50\mu s$ (half width at half maximum level, HWHM). As one can see the relaxation process follows the typical exponential law at low excitation level whereas higher power laser pulses induce TE plateau, whose maximum value relates to the state of opaqueness but the duration depends on the excitation level.

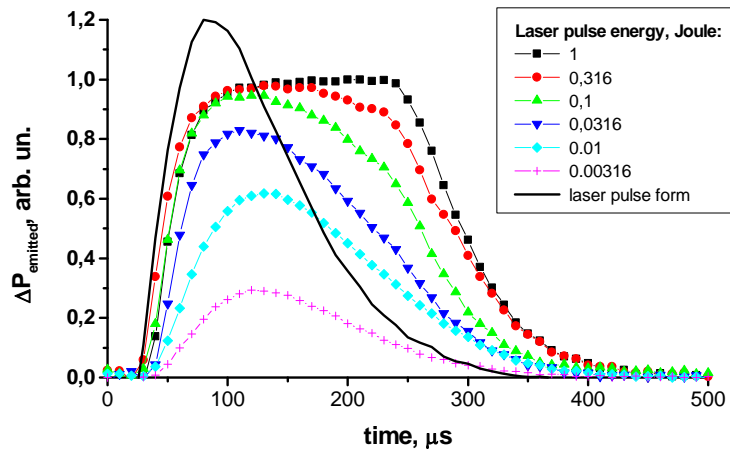


Fig.16. Ge scene ($d=5\text{mm}$, $T=195\text{C}$) transforms the value of laser power into duration of the TE relaxation process (the scene memorizes and measures the laser power). HWHM values of laser and TE pulses duration ratio depends on laser power and relate as 1:5 at higher excitation level.

In summary, intense thermal carrier generation limits application of Ge based DISP by the temperature as high as 200C . As the scene thickness should be less than carrier diffusion length, surface recombination becomes major factor limiting the device performance. Optical memory effect results in principally new property of DISP like ability to control the duration of ‘switch on’ state by varying the excitation level.

4.4. Thermal principle of photon multiplication

The fundamental background of optical transistor operation is described in Section 2.4. Here we report on the only preliminary results of experimental test of the device. Our concern were both photon (η_{phot}) and energy (η_{en}) conversion efficiencies.

Non-equilibrium scene TE was created by YAG laser and registered by piroelectric detector from the same front face. The Ge scene ($\rho=3\text{ ohm}\cdot\text{cm}$, $d=2,4\text{ mm}$, $\tau=150\text{ }\mu\text{s}$) was kept at $T=85\text{ C}$. The excitation level was rather low and related to the linear part of ‘IR TE power versus pulse laser

power” dependence, i.e. in the range of scene transparency (see Fig.15). Here we report on of the only preliminary tests.

Our results evident that quantum conversion efficiency exceeds 100% indeed ($\eta_{\text{phot}}=1,4$), i.e. each 10 photons absorbed by the scene produce 14 photons escaping the front scene face. The DISP operated in light conversion mode not only converts visible photons into IR photons but also does it with multiplication. Unfortunately, we failed to confirm another result of theoretical study. The energy conversion efficiency happened to be rather small, $\eta_{\text{en}}=0.16$ instead of predicted $\eta_{\text{en}}>1$ value. We are optimistic however about the possibility to confirm experimentally this predicted result in the nearest future. The point is that in thin scene IR TE escapes from two faces approximately in equal parts. This results in two-times increase of measured one-face value of η_{en} . The excitation wavelength may be decrease to the value $\lambda \leq 2\mu\text{m}$ (in Ge, this radiation is the most effective for carrier photo generation instead of YAG laser $\lambda=1,06\mu\text{m}$. This has to result in next two-times increase of energy conversion efficiency. The operating temperature may be increased what have to result in increase of Plank’s factor. Besides, the tests should be performed in cooled chamber in order to decrease background radiation and therefore the value of initial TE power. Finally, as we shown in Section 2.4, the recommended carrier lifetime is of some milliseconds contrary to $\tau=150\mu\text{s}$ we have had in the test. Next ways in η_{en} increasing is transparency coating and increase of total reflection angle, which is only 12° in Ge. The last means that only 2% of photons generated inside the scene escape through flat face.

In summary, remarkable properties of DISP operated in down conversion mode are the ability to multiply photons ($\eta_{\text{pho}}>1$) and to operate with energy conversion efficiency exceeding 100% (optical transistor). We experimentally demonstrated the first DISP property and figured out the way for successful test of another one.

4.5. 2D demonstration of IR images projected by the DISP

Consider in details the properties and parameters of IR image created by visible light (see details of experimental set up in Fig.9). What shown in Fig.17 is the IR image of target created at the Ge scene ($16 \times 16 \times 2\text{mm}^3$) by visible light projector. The scene front and back faces are optically polished and chemically etched. The scene itself is supported by two hot heater legs and kept at $T=84\text{C}$. The image is registered with the 8-12 μm thermal imaging camera by scanning the scene face covered with transparency coating. The IR power registered is expressed in apparent temperatures T_a and shown in false colors. In the initial state the camera “see” the scene as the object with apparent temperature $T_a = 36\text{C}$ due to low value of the scene emissivity (left frame in blue). Visible light projector provokes local increase both the scene emissivity and apparent temperature ($T_{\text{max}}=65,4\text{C}$) and creates the image (frame in center in green). By subtracting the frames one can get the IR 2D image of the target ($\Delta T_{\text{max}}=29,4\text{C}$, right frame red).

We have to remember that contrary to the majority of know to date DIPS engines all the shanges across the scene originates from its emissivity dynamic modulation wthereas the real scene temperature is kept constant. Therefore, this device time response is originated by free carrier recombination–generation processes (microsecond range) in the semiconductor scene but not the Joule heating and cooling processes (millisecond range) which are dependent on a pixel thermal mass and thermal conduction. Also by this reason, this scene spatial resolution is subjected by carrier lateral diffusion. By varying the scene parameters (doping level, surface treatment), the spatial resolution scatters between $100\mu\text{m}$ and 1mm . The maximum

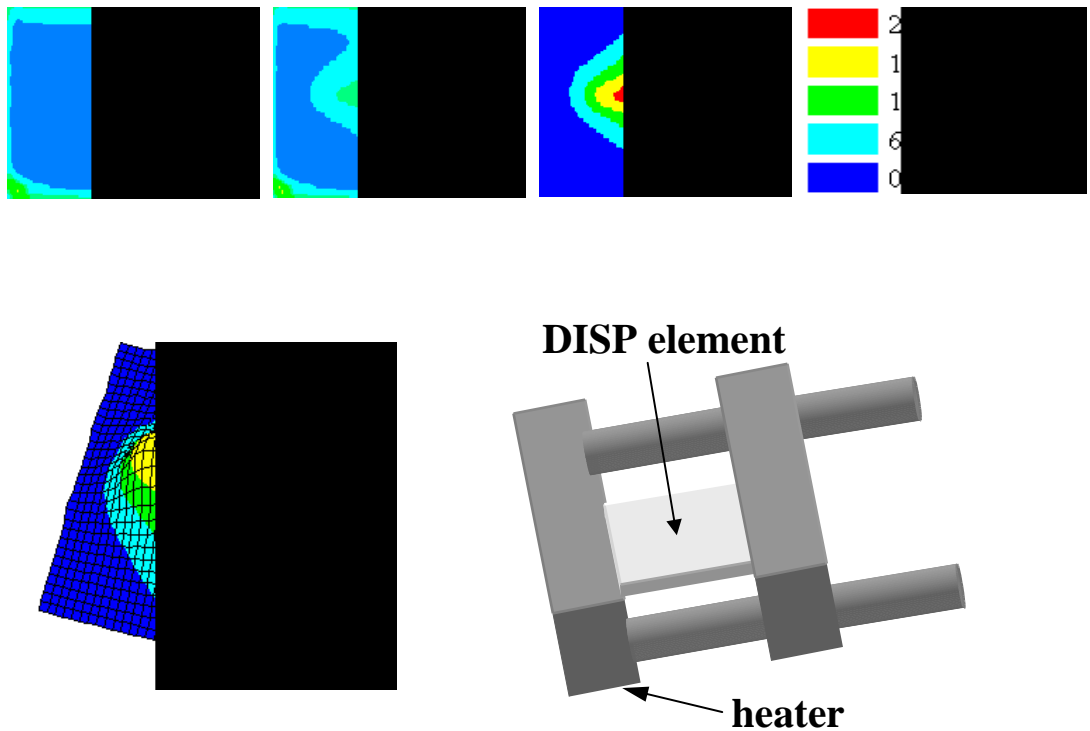


Fig.17. Top, from the left to the right: 2D distribution of apparent temperature T_a simulated by non irradiated and irradiated scenes, and these frames difference ΔT_a . Legend shows apparent temperature scale only for last for subtracted image. Down: 3D IR image of target (cross) and the scene design.

dynamically simulated temperature is real scene temperature provided the pumping power is capable to provoke the scene opaqueness (what is not the case in our example). The temperature range is the temperature difference between the scene (which can be heated up to melting temperature) and the background as the initially transparent scene permits the background radiation to pass through the scene and be registered by the camera.

There is another possibility of practical application of down conversion principle in DISP devices. Contrary to the approach described, the target is not projected by visible light but exists on the scene a priori. The forming the region whose emissivity differs the scene emissivity can create this target, for example by conventional lithography method. In this case, the visible light only changes the target emissivity (by generating free electrons and holes and therefore increasing the absorption coefficient of irradiated region) and thus provokes dynamic difference between apparent temperatures of a target and scene.

More specifically we covered the thin Ge scene (with emissivity as low as $\epsilon=0,1$) with bismuth film whose emissivity was about $\epsilon= 0,35$. The target (aircraft) was created at Ge surface by conventional lithography and etching. As a matter of fact it was Ge surface free of bismuth film. In such a case the target was seen by camera as a cold object (see Fig.18). Visible light provoked both target emissivity increase and new apparent temperature difference between the target and scene. It is to point out that we have managed to dynamically “erase” the target or simulate both cold and hot target at the given point of the scene.

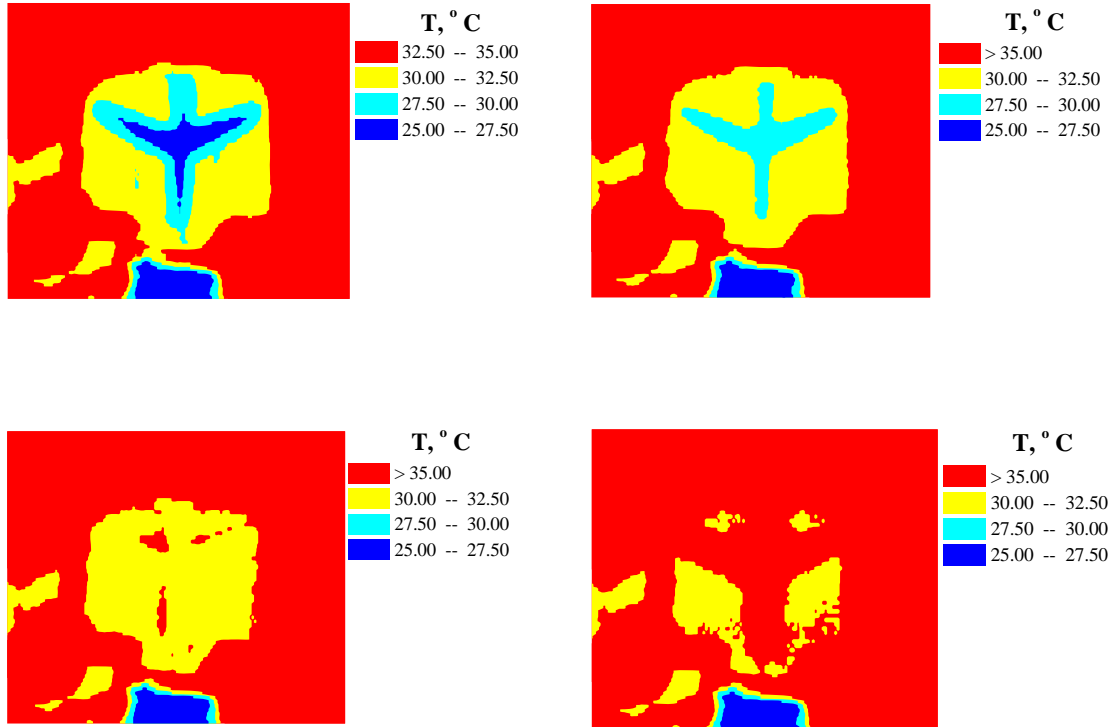


Fig.18. Down-conversion DISP simulates Stealth effect. Red is hot screen, yellow is the scene, and blue is target. Top left-initially cold target ($T_t - T_s = -5C$) created by scene emissivity pattern, top right-low level visible light decreases the target contrast ($T_t - T_s = -2,5C$). Down left- relevant level visible light erases the target ($T_t - T_s = 0$), only some kind of noise is available on the frame), and down right-high level visible light transforms cold target into hot target ($T_t - T_s > 5C$).

It is important to point out that the possibility exists to create at the scene numerous targets with different initial temperatures, whose apparent temperatures could be dynamically simulated or erased.

In summary, two different approaches (both utilize down conversion DISP device and scene emissivity modulation, the scene temperature is kept constant) were experimentally demonstrated. The first one is able to transform visible ‘movie’ projected at the uniform semiconductor scene into visible from all sides IR ‘movie’ whose ‘stars’ however are reluctant to demonstrate negative apparent temperatures. The second device contains test picture ‘written’ on the scene by different colors-local emissivity values. By irradiating the scene with uniform light it is possible to create the image with negative and positive temperatures. Moreover, the initially written image may be dynamically erased. In both cases, the spatial resolution is limited by free carrier diffusion length and time response is comparable to carrier lifetime. The scene temperature is kept constant.

4.6. 3D DISP device concept

Till now we had been discussing the modulation of scene emissivity (through free carriers generation) by irradiating its surface with visible light. Suppose we create free carriers in any way inside the scene. As the scene is initially transparent, the camera registers uniform low temperature object in initial state but has to register excess temperature in the point where free carriers appear. It is important to note that the local temperature non-uniformity will be seen by camera from all directions and faces.

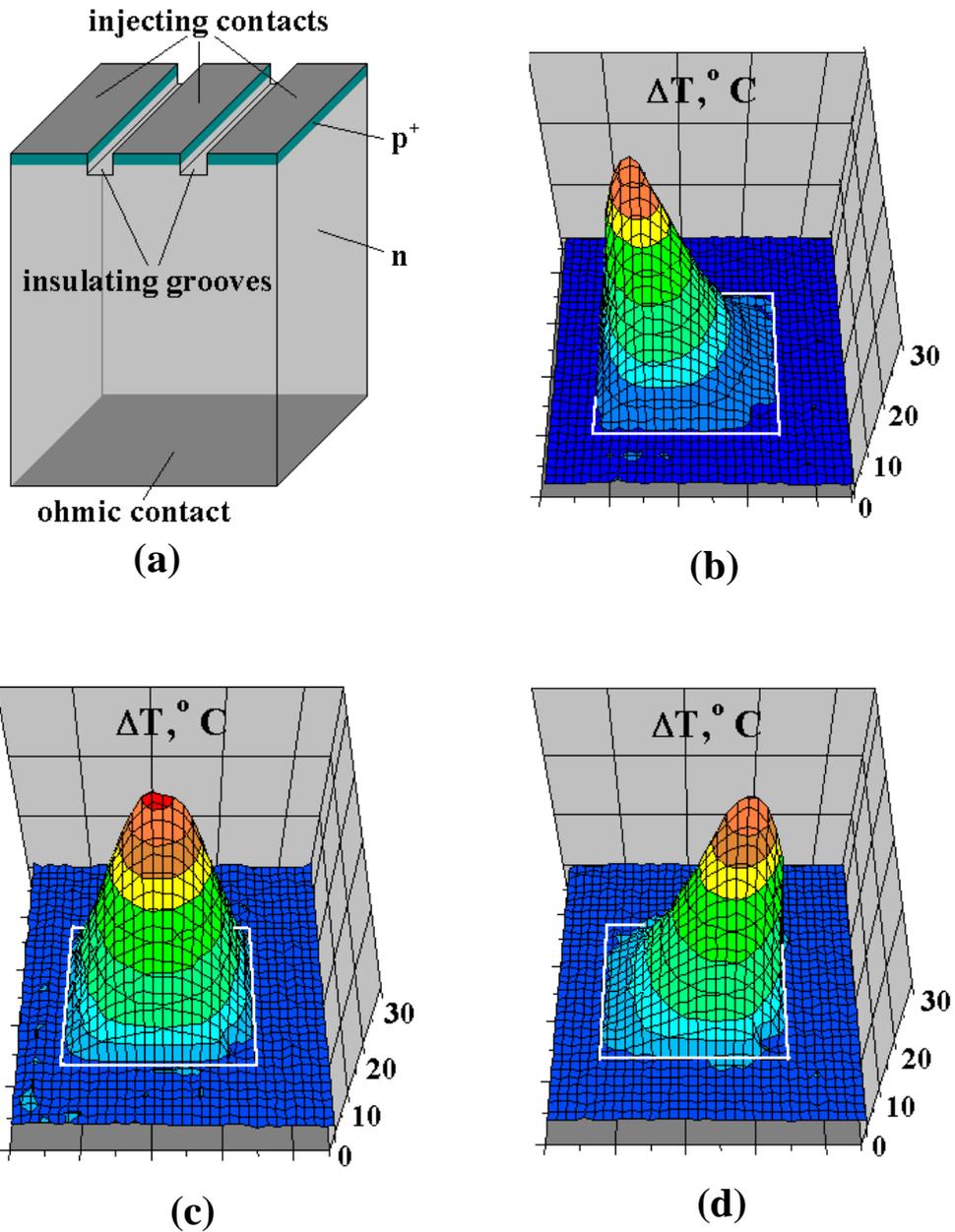


Fig.19. IR camera captures three different stripes of practically uniform 3D distribution of power emitted by the scene with biasing current value being operating parameter. The maximum apparent temperatures are seen in the vicinity of p-n junction. Images (b) and (d) are not symmetric due to surface recombination impact.

In our experiments, local non-transparency of Ge scene was provoked by carrier contact injection through p-n junction (see Fig.19). P-n junction itself was divided by insulating grooves into three stripes. Another contact to the base was patterned ohmic contact (see Fig.19a). By manipulating the number of active stripes, IR emission could be simulated from the left (b, left p-n junction is biased), in the center (c, next junction is biased), and from the right (d, right junction is biased). The $5 \times 5 \times 8 \text{ mm}^3$ scene was kept at $T=83\text{C}$, maximum apparent temperatures values $\Delta T, ^\circ\text{C}$ were: b-25,9 c- 27,7 and d- 26,8. IR camera scans the scene from the front plate, pulse (160ms) driving current value is $I=A$. Different 3D-echelons of IR light at the IR scene are clearly seen.

In summary, the unique property of DISP device is its initial transparency in IR. Thus, 3D image created inside the scene by modulating its local emissivity will be seen by camera from all the direction. Its position in x-y-z coordinates can be localized by conventional tomography approach. We demonstrated 3D image by carrier injection in local scene cross section. The same can be done also by projecting at the scene two (or more) laser beams. These beams have to cross each other inside the scene and produce local carrier generation increase i.e. hot spot.

4.7. Patent pending

Results of the work were arranged as patent pending registered in Ukraine and the US. What follow below is short resume of our proposals.

Device for generation of dynamic 2-dimensional infrared images^{6,7}

The following device can be used for the generation of dynamic 2-dimensional infrared images and testing of optical systems that work in the infrared range.

The device also contains projector of optical emission and conversion screen that can be found on optical axis of the projector. Moreover, screen intensity modulation is done using the characteristics of a semiconductor material plate, in which, the width of the semiconductor forbidden zone is smaller than the optical emission quantum energy, and as well as, ways for maintaining the operational temperature.

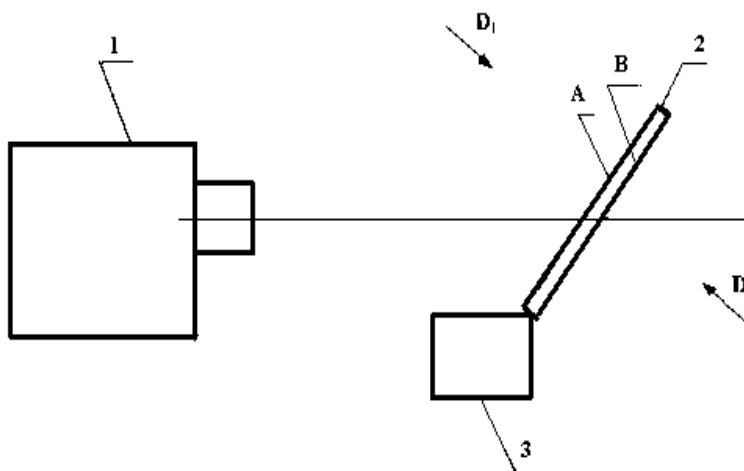


Fig.20. General layout. 1 -optical radiation projector, 2 - conversion screen, 3 - temperature maintaining device. A is the front surface of the conversion screen, B is the opposite (rear) side of the conversion screen. Observation of the infrared images can be done in the D1 or D2 direction.

The offered device provides for the reduction of thermal inertia; increase in spatial resolution; increase in the maximum resolution and dynamic range of the temperatures that are being represented; increase in mechanical durability and reliability of the device; as well as expansion of it's functional possibilities; and especially representation of temperatures lower than the temperature of the background. Fig.20 presents the general schematic view of the device. The device contains an optical radiation projector - 1, a conversion screen -2, an operational temperature-maintaining device - 3. A is the surface of the conversion screen - 2, that is facing optical emission projector -1; B is the opposite side of the conversion screen - 2. Observation of the infrared images can be done in the D1 or D2 direction.

Method for simulation of infrared scene with controlled thermal contrast⁸

The invention relates to infrared (IR) engineering and can be used for simulation of IR scenes with controlled thermal contrast in the IR radiation wavelength range from 3 up to 20 micrometers, in particular, for testing IR devices. According to the method, a metal layer is deposited onto a semiconductor material plate, a local action is made on this layer to form scene elements geometrically similar to those preset, and control is exerted over contrast of the IR scene (made by intrinsic radiation from the semiconductor surface and metal areas) through variation of the free charge carrier concentration in the semiconductor material by irradiation of the semiconductor plate with photons whose energies are over the semiconductor material band gap, thus making it possible to expand functional capabilities for IR scene simulation through intrinsic radiation from the elements that form images of these scenes, in particular, to essentially increase the rate of controlled variation of their thermal contrast.

P.S. By our proposal the duration of this work was extended by two months without additional funding. The reason: it was urgent need to prepare set of materials for the petition to the Ukrainian patent office (second patent pending). This work was not scheduled by initially approved working plan and was not supported financially by the Partner.

4.8. Independent testing, reporting, and publishing the results

This project manager visited AFRL (Eglin, FL) in April this year to discuss ongoing joint research effort with the Air Force Research Laboratory and to perform common tests of the devices developed^{9,10} (see Fig.21-22).



Fig.21.Common tested started in Eglin area, FL⁹

The main purpose was to demonstrate the physical principle of the devices and reproduce the results of the tests performed in Kiev. Details of simulating negative temperatures as well as scientific based understanding of extreme temperature differences between the scene and background were also on the agenda.

Results of this work were reported at CREOL School of the University of South Florida (Orlando) and general presentation was made to the Emerald Coast Optical Society at the University of Florida Graduate Engineering and Research Center (FL). Scientific presentation was made also at the International Symposium on Optical Science and Technology (SPIE's 47th Annual Meeting^{11,12}) and is to be reported at the MIOMD-V International conference (Annapolis, September 8-11, 2002)¹³.

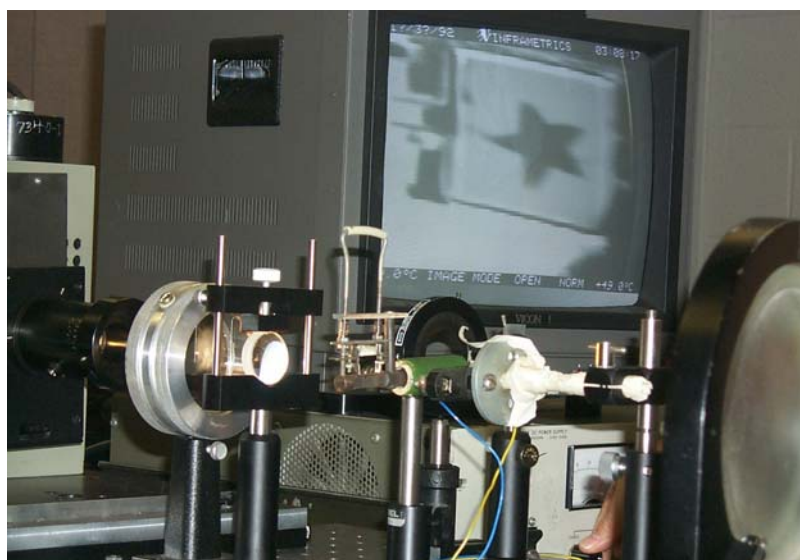


Fig.22. Test Set Up- Oriel 150W Light Engine From the left, Water Filter to remove IR, Condenser Lens, Holder with Germanium Sample and collimator lens for IR camera. Monitor with IR Star Image and Heater Power Supply in Rear (Eglin AFB, Florida, USA).

5. Conclusions

The emissivity (and apparent temperature) modulation of an optically thin heated semiconductor screen, which is directly followed by modulation of IR radiation emitted (light down conversion), is a direct effect of non-equilibrium free current carrier generated by the visible pumping. Free electrons and holes generate an increase of absorption coefficient and the scene opaqueness in IR. Phonon assisted non-direct electron transitions in the conduction band and direct hole transitions between sub-bands of the valence band form different values of absorption cross sections ($\sigma_n < \sigma_p$) thus, intentional doping of the IR scene is a factor of DISP quality. A few mW/cm^2 appear to be typical values of dynamically modulated IR power emitted by the scene kept at reasonably high temperatures ($T < 450\text{K}$). As a matter of fact this works creates principally new approach in DISP design.

Free carrier absorption induces a dynamic increase of semiconductor emissivity over the whole IR spectral range. It should be mentioned that the maximum TE modulated power falls into the near and mid IR (3-20microns). Secondly, this device time response is controlled by free

Tabl.2. Down conversion DISP versus MIRAGE engine (SBIR)

	<i>PARAMETERS</i>	<i>MIRAGE (SBIR)</i>	<i>CONVERTER</i>
1	Operation principle	Equilibrium BB radiation	Visible-to IR down conversion
2	Emitter	Resistive heater /micro-array/	Semiconductor screen
3	Time constant	5 ms, thermal process	<100μs, recombination process
4	Key factor	Temperature, T	Emissivity, ϵ
5	Effective temperature range	286-780 K	250-780 K (projected)
6	Fill factor	46,5%	100%
7	Temperature contrast	$\Delta T > 0$, simulate hot objects	$\Delta T > 0$, $\Delta T < 0$, hot and cold objects
8	Cross talk	Minimum (?)	Carrier diffusion length
9	Information source	Row-column addressing Si read-in integrated circuit	Image projected by visible light
10	Frame rate	200 Hz	200-20 kHz
11	Efficiency	<100%	>100%, (predicted)

carrier recombination–generation processes (microsecond time range) in the semiconductor screen and not the Joule heating and cooling processes (millisecond range) in current IR displays which are dependent on a pixel thermal mass and thermal conduction. Also, it is significant that only semiconductor melting temperature limits the possible maximum dynamically modulated apparent temperature values. In addition there are not any driving electronics that demands large cumulative current and power and heat the substrate and package. Fill factor is determined only by the spread function of the carrier diffusion and the point spread function of the visible light projector.

It is important to note that key results of this work were investigated in the USA. These independent tests don't contradict to these work conclusions.

Two new properties of DISPs were proposed and studied in this work. The first, it was shown that down conversion DISP devices are capable to memorize the value of visible power emitted through time response versus visible power dependence (optical memory effect). The second, it was shown that DISP device might operate with energy conversion efficiency exceeding 100%. Also the possibility to simulate both cold and hot target (though is not new) should be mentioned. For detailed comparisons of down conversion DISP versus most elegant DISP available in the market (Santa Barbara IR Emitter Array Projector¹⁴) see Tabl.2.

Looking ahead, some proposal to push this problem toward forward might be outlined. The first, our study shows that Ge scene can be successfully operated only at low simulating temperature ($T \leq 200^{\circ}\text{C}$), which is limited by high rate of carrier thermal generation. Next contender is obvious. It should be Si. By the preliminary estimates, Si based DISP have to cover temperature range up to $T \approx 500^{\circ}\text{C}$. Future study might be targeted on wide band semiconductors like 11-VI compounds.

The second, optical transistor operated in heat pump mode looks attractive from both fundamental and practical points of view. Really, the possibility to transform waste heat into directed light energy worth to be studied in details as a separate work.

The third, it is not clear till now what is the range of negative temperatures, which DISP can simulate. This work evidences that TE modulation can produce negative contrast like negative luminescence already described in literature. But comparative tests like TE versus negative luminescence have not been performed yet.

6. Acknowledgment

This work was performed in cooperation and under financial support of the Air Force Research Laboratory Munitions Directorate and Air Force European Office of Aerospace Research and Development. We appreciate the attention and support of Colonel Gerald O'Connor, Prof. M. Stickley, and Dr. Alex Glass from EOARD (London) and Dr. L. Taranenko and Mr. B. Rovinski from STCU (Kiev).

7. References

1. Owen M. Williams, " Dynamic infrared scene projection: a review", *Infrared Physics & Technology* **39**, pp. 473-486, 1998.
2. V. K. Malyutenko, "Thermal emission in semiconductors. Investigation and application", *Infrared Physics*, **32**, pp. 291-302, 1991
3. M. Vasil'eva, L. Vorobyev and V. Stafeev, *Fiz. Thechn. Polupr.* **1**, pp.29-33, 1967
4. T.S. Moss, "Photon pressure effect in semiconductors", *Phys.stat.sol. (a)* **8**, pp. 223-232, 1971
5. D.L. Stierwalt and R.F. Potter, " Infrared spectral emittance of Si, Ge and CdS", *Pros. Intern. Conf. on the Physics of Semiconductors*, Exeter, July 1962,pp.513-520
6. V.K. Malyutenko, J.R. Kircher, R.L. Murrer, Jr., O.Yu. Malyutenko, V.V. Bogatyrenko. Ukrainian Patent Disclosure Number 2000095565, Sep. 28, 2001.
7. V.K. Malyutenko, R.L. Murrer, Jr., J.R. Kircher, D.R. Snyder, III, O.Yu. Malyutenko, V.V. Bogatyrenko. USAF/ISP Joint Patent Disclosure Number D00601, May 2002.
8. V.K. Malyutenko, D.R. Snyder, O.Yu. Malyutenko, E. V. Michailovskaya, V.V. Bogatyrenko. Ukrainian Patent Disclosure Number 2002064925, July 14, 2002
9. *Eglin Eagle Newspaper*, **61**, N13, p.8 (April 5, 2002)
10. *News@afrl*. The official voice of the Air Force Research Laboratory, May 2002
11. V.K. Malyutenko, V.V. Bogatyrenko, O.Yu. Malyutenko, D. R. Snyder, A.Huber, J. Norman, " Semiconductor Screen Dynamic Visible to Infrared Scene Converter", *SPIE's 47th Annual Meeting 7 - 11 July 2002*, Seattle, WA, USA.
12. V.K. Malyutenko, V.V. Bogatyrenko, O.Yu. Malyutenko, D.R. Snyder, A. Huber, J. Norman " Semiconductor Screen Dynamic Visible To Infrared Scene Converter", *Pros. SPIE*, **4818**, 2002, in press.
13. V.K. Malyutenko, K.V. Michailovskaya, O.Yu.Malyutenko, V.V.Bogatyrenko, D.R. Snyder "Pixelless IR Dynamic Scene Simulating Device", %th International conference on Mid-infrared Optoelectronics Materials and Devices, Annapolis-2002
14. R. Robinson, J. Oleson, L. Rubin and S. McHugh, "MIRAGE: System overview and status," *Pros. SPIE* **4027**, pp. 387-398, 2000.